

# Beryllium parabolic refractive x-ray lenses

B. Lengeler<sup>a</sup>, C. G. Schroer<sup>a,b</sup>, M. Kuhlmann<sup>a</sup>, B. Benner<sup>a</sup>, T. F. Günzler<sup>a</sup>, O. Kurapova<sup>a</sup>,  
F. Zontone<sup>c</sup>, A. Snigirev<sup>c</sup>, and I. Snigireva<sup>c</sup>

<sup>a</sup>II. Physikalisches Institut, Aachen University, D-52056 Aachen, Germany;

<sup>b</sup>HASYLAB at DESY, Notkestr. 85, D-22607 Hamburg, Germany;

<sup>c</sup>European Synchrotron Radiation Facility ESRF, BP 220, F-38043 Grenoble, France

## ABSTRACT

Parabolic refractive x-ray lenses are novel optical components for the hard x-ray range from about 5 keV to about 120 keV. They focus in both directions. They are compact, robust, and easy to align and to operate. They can be used like glass lenses are used for visible light, the main difference being that the numerical aperture  $NA$  is much smaller than 1 (of order  $10^{-4}$  to  $10^{-3}$ ). Their main applications are in micro- and nanofocusing, in imaging by absorption and phase contrast. In combination with tomography they allow for 3-dimensional imaging of opaque media with sub-micrometer resolution. Finally, they can be used in speckle spectroscopy by means of coherent x-ray scattering. Beryllium as lens material strongly enhances the transmission and the field of view as compared to aluminium. With increased  $NA$  the lateral resolution is also considerably improved with Be lenses. References to a number of applications are given.

**Keywords:** synchrotron radiation, refractive x-ray lenses, beryllium, x-ray imaging, x-ray microscopy, tomography, x-ray microprobe

## 1. INTRODUCTION

In this paper, we report on the status of refractive x-ray lenses with rotationally parabolic profile manufactured from beryllium. Refractive x-ray lenses have been considered for a long time as not feasible, due to the weak refraction and the relatively strong absorption of x-rays in matter. However, in 1996 we could show experimentally that focusing by x-ray lenses is possible if the radius of curvature  $R$  of the lenses is chosen small (below 0.5mm), if many lenses are stacked behind one another in a row, and if a lens material with low  $Z$ , like aluminium, is chosen.<sup>1,2</sup> The first lenses consisted of a row of holes, 1mm in diameter, drilled in a block of aluminium. Two of these lenses in crossed geometry were able to focus the x-ray beam from an undulator source to a spot size of a few  $\mu\text{m}$ .

## 2. ROTATIONALLY PARABOLIC REFRACTIVE X-RAY LENSES

In the meantime, we have developed at Aachen University lenses with rotationally parabolic profile.<sup>3-5</sup> This allows for focusing in both directions, free of spherical aberration and other distortions. An excellent candidate as lens material is beryllium. Its low value of  $Z = 4$  reduces absorption substantially compared to aluminum ( $Z = 13$ ). Having been able to solve the problems with handling and plastically deforming beryllium, we currently manufacture Be lenses with rotationally parabolic profile.<sup>6</sup> The Be blanks were purchased from Brush Wellman Inc. Figure 1(a) shows a stack of Be lenses in their casing with protective atmosphere (in order to avoid oxidations of the Be by ozone in the x-ray beam). Figure 1(b) shows a schematic drawing of an individual lens. Note the concave shape of a focusing lens, which is a result of the diffractive part  $1 - \delta$  of the index of refraction  $n$  being smaller than 1.

In the thin lens approximation, the focal length of a stack of  $N$  lenses is  $f = R/2N\delta$ . Here,  $R$  is the radius of curvature at the apex of the paraboloid. For paraboloids,  $R$  and the geometric aperture  $2R_0$  are independent of one another, in contrast to the case for spherical lenses. We typically choose  $R = 0.2\text{mm}$  and  $2R_0 = 1\text{mm}$ .

---

Further author information: (Send correspondence to B. Lengeler)

B. Lengeler: E-mail: Lengeler@physik.rwth-aachen.de, Telephone: +49 (241) 80 27077

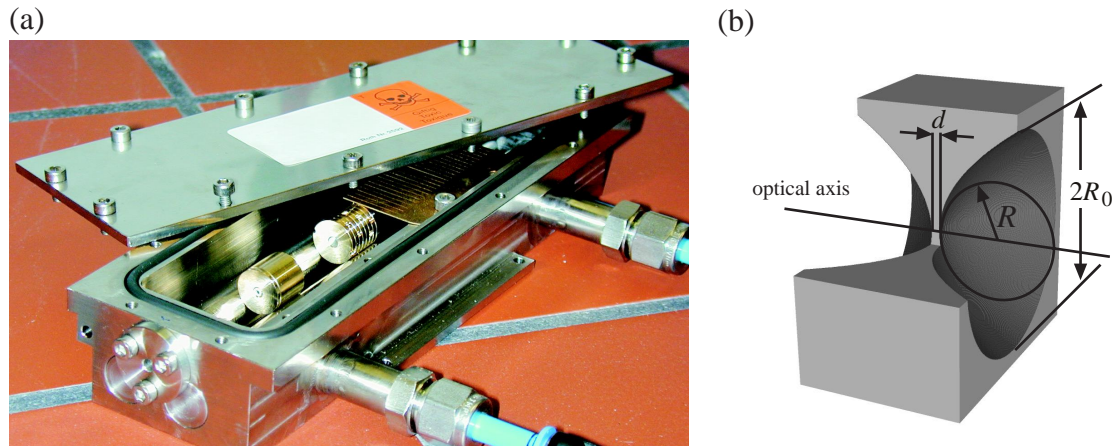


**Figure 1.** (a) partly assembled Be lens. (b) schematic drawing of an individual refractive x-ray lens.

The thickness  $d$  of the material between the apices of the paraboloids is about  $50\mu\text{m}$  for Be, but can be made as thin as  $25\mu\text{m}$ . Up to  $N = 300$  lenses can be aligned in a lens stack in such a way that the optical axes of the individual lenses agree on the micrometer scale. The form fidelity of the paraboloids is better than  $0.3\mu\text{m}$  and surface roughness is below  $0.1\mu\text{m}$ . Parabolic surfaces turned out to be smoother than spherical surfaces because parabolic indentation tools generate normal forces everywhere along the profile.<sup>7</sup>

Compared to mirrors, refractive lenses are about a factor of 1000 less sensitive to surface roughness. Roughness induced damping in the transmission is proportional to  $\exp(-Q^2\sigma^2)$ . The momentum transfer  $Q$  in a mirror with critical angle  $\vartheta_c = 0.3^\circ$  at  $1\text{\AA}$  wavelength is  $Q = 7 \cdot 10^{-2}\text{\AA}^{-1}$ . In a lens stack with  $N = 100$ ,  $Q$  is only  $1.4 \cdot 10^{-4}\text{\AA}^{-1}$ , which is smaller by a factor 500. Hence, the lens can allow for a 500 times increased surface roughness  $\sigma$  for the same damping. This is an important aspect in the production process of the lenses. It turned out that surface roughness plays no role in imaging by our refractive x-ray lenses.

It often happens that the total length  $L$  of a lens stack is not negligible compared to the focal length  $f$ . For instance, at  $15\text{keV}$ , the value for the index of refraction decrement  $\delta$  in Be is  $1.515 \cdot 10^{-6}$ . For a stack of  $N = 300$  individual lenses and for  $R = 0.2\text{mm}$ , the focal length  $f_0$  in the thin lens approximation is  $0.220\text{m}$ , compared to a length  $L$  of  $0.300\text{m}$ . Here, the focus is measured from the middle of the lens. In the thick lens approximation, the focal length is<sup>8</sup>

$$f = f_0 \frac{1}{1 - \frac{1}{6} \frac{L}{f_0}} = 0.220\text{m} \cdot 1.294 = 0.285\text{m} \quad (1)$$

The principal plane  $H_2$  is shifted by  $-\frac{1}{24}L^2/f_0$  from the center of the lens, which, in the present case, is  $0.017\text{m}$ . Hence, the focus is located at  $0.118\text{m}$  from the end of the lens (compared to  $0.070\text{m}$  in the thin lens approximation). This estimation shows that the thin lens approximation gives only a rough value of the focal length and that the lens has to be considered as thick in most cases of interest for refractive x-ray lenses.

The attenuation of x-rays in matter is a key parameter in the design of refractive x-ray lenses. Figure 2 shows the mass absorption coefficient  $\mu/\rho$  for Be, Al and Ni. At low energies (below about  $10\text{keV}$ ), attenuation is dominated by photoabsorption,  $\tau/\rho$ , which varies approximately like  $Z^3/E^3$  with atomic number  $Z$  and with photon energy  $E$ . Below about  $0.15\text{cm}^2/\text{g}$  the attenuation coefficient stays basically constant, independent of energy and atomic number  $Z$ . This happens when Compton scattering starts to dominate the attenuation coefficient. Compton scattering ultimately limits the performance (lateral and longitudinal resolution) of refractive x-ray lenses. Compton scattering has a twofold detrimental influence. Photons which are Compton scattered do no longer contribute to the image formation. In addition, they generate a background in the detector which reduces the signal to background ratio in the image.

Synchrotron radiation sources of the third generation can create a considerable heat load problem in the first optical element hit by the beam. This is expected to be even more true at x-ray free-electron laser sources

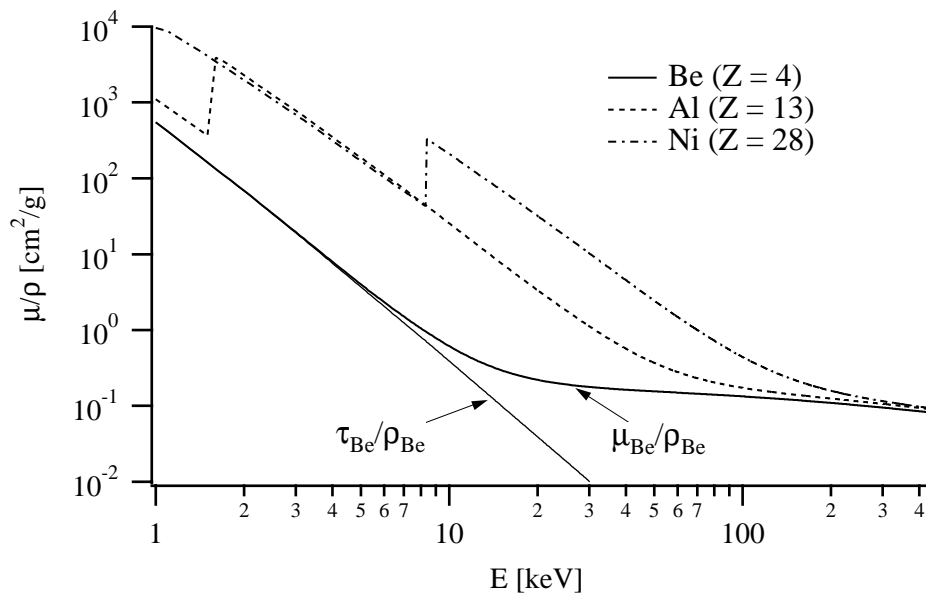


**Figure 2.** Mass attenuation coefficient  $\mu/\rho$  for Be, Al, and Ni.<sup>9</sup>

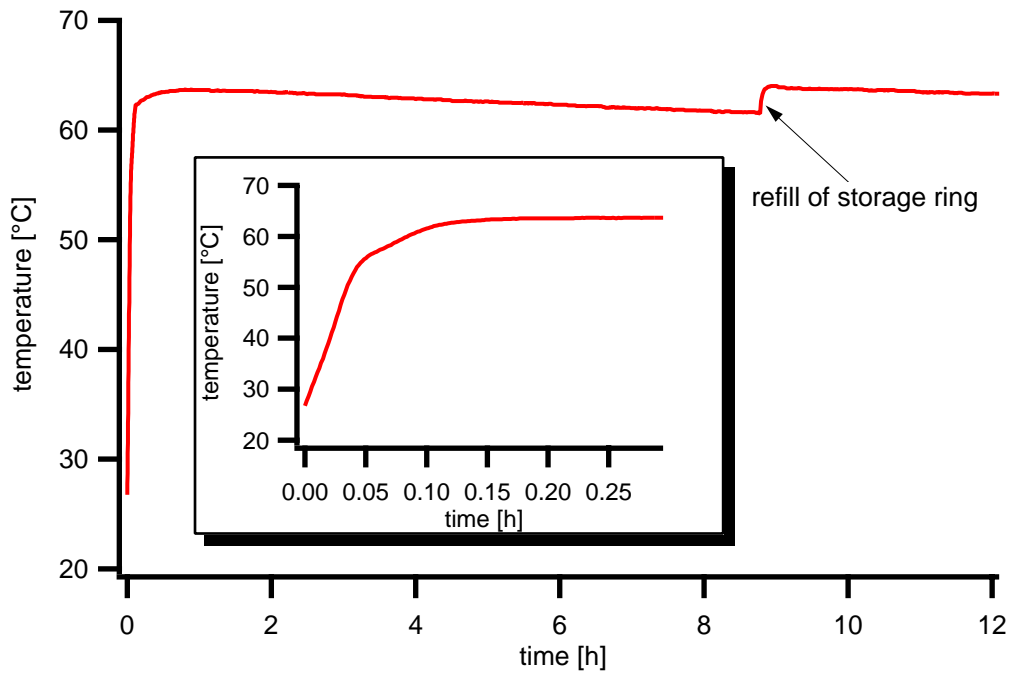


**Figure 3.** Time evolution of the temperature inside a beryllium lens that is illuminated by the “white” beam of three undulator sources. The temperature of the beryllium of the 6th lens in a stack of 12 is measured by a thermocouple as a function of time after opening the beam shutter.

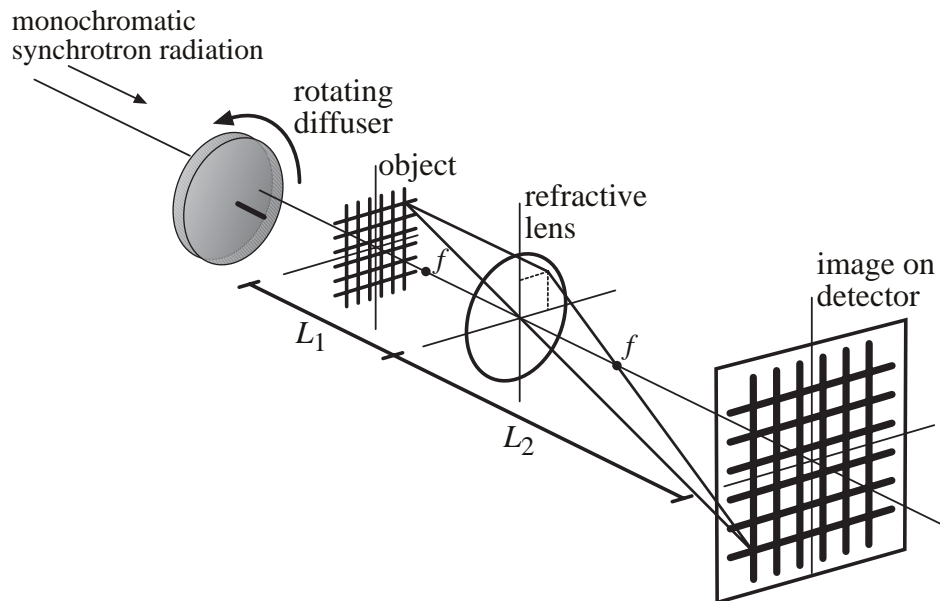


**Figure 4.** Schematic setup of a hard x-ray microscope based on parabolic refractive x-ray lenses. The sample is illuminated from behind by monochromatic x-rays. A parabolic refractive x-ray lens forms a magnified image of the object on a position sensitive detector. The diffuser reduces the lateral coherence of the illuminating beam and is used to match the beam divergence to the aperture of the objective lens.

which are developed at present. In order to test the influence of the heat load on refractive x-ray lenses we have performed a measurement at the undulator beam line ID10 at ESRF. The power density and power of the white beam generated by 3 undulators in a row was about  $100\text{W}/\text{mm}^2$  and  $40\text{W}$ , respectively. A stack of 12 Be lenses was exposed to the beam. The lenses were housed in an evacuated casing. They were indirectly cooled via a thermal link to a copper plate which was water cooled. The temperature was measured by 3 thermocouples, one at each end and one in the middle of the lens stack. The highest temperature was measured in the middle. The temperature-time profile is shown in Figure 3. The temperature increases within about 15 minutes to  $65^\circ\text{C}$  and stays constant afterwards, except for small variations due to changes of the electron current in the ring. A temperature of  $65^\circ\text{C}$  poses no problem for the Be lenses. The melting point of Be is at  $1285^\circ\text{C}$  and recrystallization of Be occurs only above  $600^\circ\text{C}$ . In other words, refractive Be lenses can cope with the heat load of third generation synchrotron radiation sources and very likely also do with that at x-ray free-electron lasers.<sup>10-13</sup> Whether photodesorption in the high electric field of a laser beam will create problems has to be tested when these sources become available. At the present undulator beam lines no deterioration of Be or Al x-ray lenses has been observed, even after years of operation. Metallic lens materials are far superior to insulators, like plastics or glass. The high density of free electrons in metals prevents radiation damage by bond breaking or local charging.

### 3. IMAGING WITH PARABOLIC REFRACTIVE X-RAY LENSES

Refractive x-ray lenses with parabolic profile can be used in a hard x-ray microscope. When the object, illuminated with monochromatic x-rays from an undulator beamline, is located (at  $L_1$ ) slightly outside of the focal length  $f$ , then a magnified image is generated at  $L_2$  with  $L_2 \gg f$ . Figure 4 shows a typical set-up for an x-ray microscope. The object, illuminated from the backside by a monochromatic x-ray beam, is positioned slightly outside the focal point. Then a magnified image is generated at a distance  $L_2$  from the lens. The magnification  $M = L_2/L_1 = f/(L_1 - f)$  can be up to 100. Figure 5(a) shows the image of a Ni grid (mesh 2000 with period  $12.7\mu\text{m}$ ) imaged with a Be lens ( $N = 91$ ,  $f = 493\text{mm}$ ,  $L_2/L_1 = 10$ ) at 12 keV onto high resolution x-ray film. Details of the contrast formation are described in.<sup>14, 15</sup> There are no distortions visible in the image.

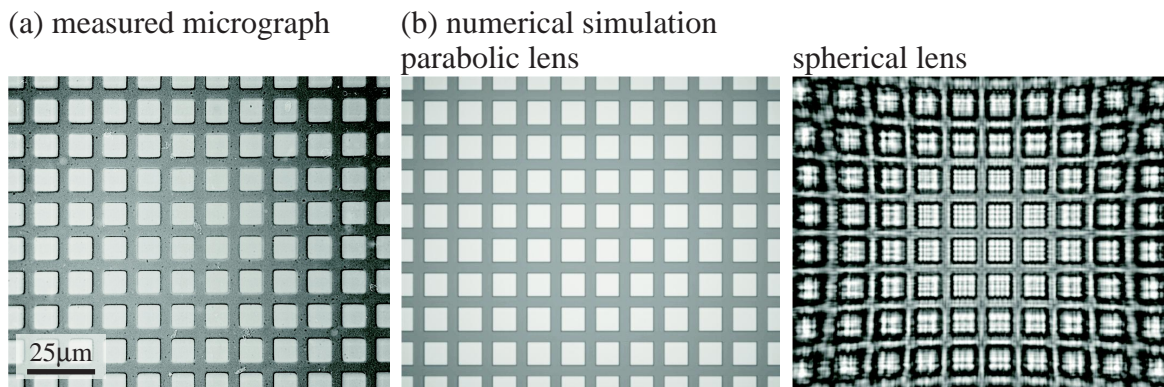


**Figure 5.** (a) hard x-ray micrograph of a Ni mesh.<sup>6</sup> (b) Numerical simulation of the imaging process using a parabolic and spherical lens.

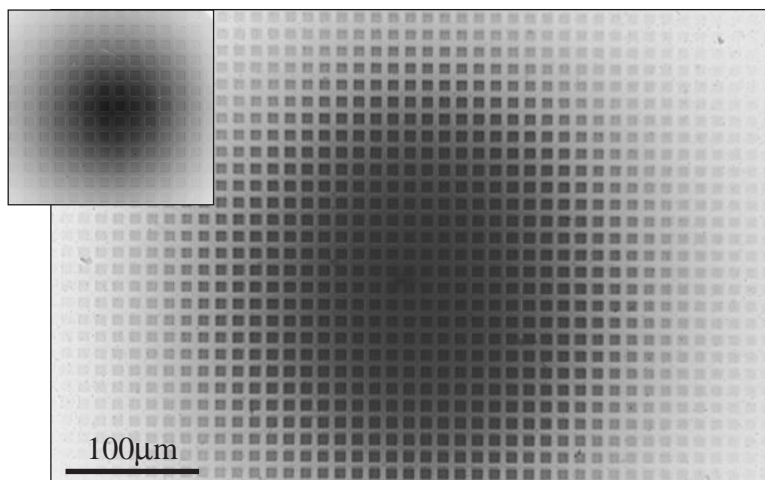


**Figure 6.** X-ray micrograph of a Ni mesh (2000mesh) recorded at 12keV in 10 $\times$  magnification using a Be refractive lens.<sup>6</sup> The field of view is about 450 $\mu$ m (FWHM), but over 550 $\mu$ m can be used for microscopy. For comparison, the same Ni mesh imaged by an Al lens at  $E = 25$ keV is shown in the upper left corner. Here, the field of view is limited to 130 $\mu$ m (FWHM), but over 160 $\mu$ m can be used for microscopy.

This is a consequence of the parabolic lens profile. Fig. 5(b) compares imaging with parabolic and spherical lenses in a numerical simulation. Spherical aberration dominates the image formed by the spherical lens, clearly demonstrating the need for a lens surface in the form of a paraboloid of rotation.

Beryllium as lens material has 2 major advantages compared to aluminium. First, the field of view is enlarged and secondly, the lateral resolution is improved considerably. Figure 6 illustrates the increase in the field of view when Be rather than Al is chosen as lens material. For the present Be lens ( $E = 12$ keV,  $N = 91$ ,  $f = 0.495$ m) the field of view is 550 $\mu$ m compared to 150 $\mu$ m for Al ( $E = 25.5$ keV,  $f = 1.05$ m). In some cases with smaller magnification the effective aperture can be as large as 900 $\mu$ m.

Up to now, we have achieved a lateral resolution of 100nm in x-ray microscopy with our Be lenses. This is shown in Figure 7. A gold structure with a period of 2 $\mu$ m, a line width of 1 $\mu$ m and a thickness of 2 $\mu$ m was used as a test object. A stack of 91 Be lenses with a focal length of 495mm at 12keV and a magnification of 10 generated the image on a high resolution x-ray film. After correction for the film granularity a resolution of 105nm was achieved, compared to an expected resolution of 84nm.

The question arises what is the limit of lateral resolution,  $d_t$ , which can be achieved with refractive x-ray



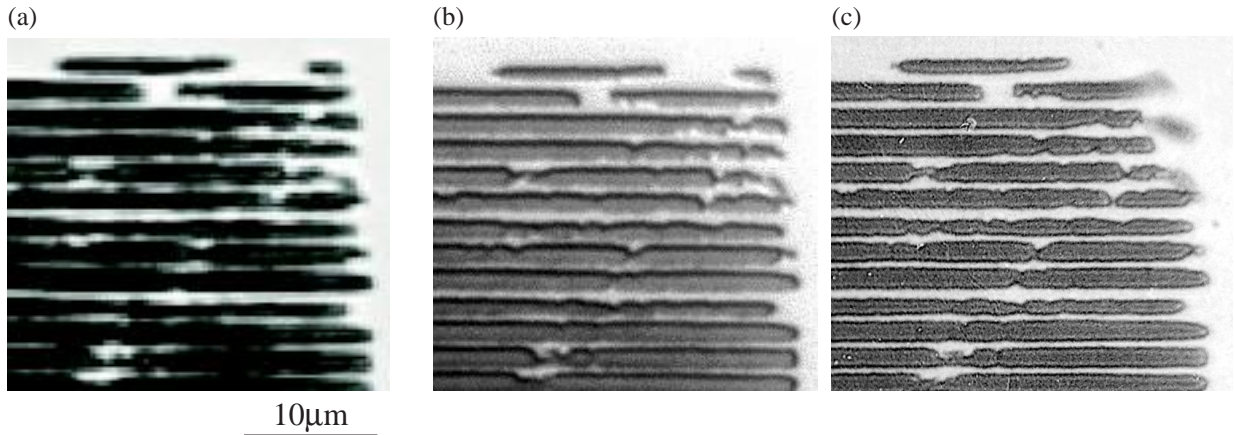


**Figure 7.** (a) Projection image of a test pattern made of (imperfect) gold stripes on a silicon substrate recorded in parallel projection by a high resolution x-ray camera (FReLoN2000) at  $E = 20\text{keV}$ . (b) x-ray micrograph of the same sample recorded at  $24.9\text{keV}$  in  $21\times$  magnification using an aluminium refractive lens. (c) x-ray micrograph recorded in  $10\times$  magnification at  $12\text{keV}$  using a beryllium objective lens. Some of the structures in the upper right corner in (a) and (b) were damaged prior to recording the image shown in (c).

lenses, in particular, is it possible to achieve atomic resolution. In the following, we will give arguments showing that with the present technology in lens fabrication it will be difficult to reach a resolution below  $30\text{nm}$ . We believe that atomic resolution cannot be achieved. Indeed, the uncertainty principle gives for the lateral resolution a value of

$$d_t = 0.75 \frac{\lambda}{2NA} = 0.75 \frac{\lambda}{2 \sin \alpha}. \quad (2)$$

The numerical aperture  $NA$  is given by  $\sin \alpha$ , where  $2\alpha$  is the angle spanned by the effective aperture of the lens as seen from an object point.<sup>4</sup> This result is well known from optics, the prefactor 0.75 being different from the usual factor 1.22. The difference can be traced back to the fact that in normal optics apertures are sharply delimited whereas in x-ray optics the attenuation smears out the boundary of an aperture. We now estimate the value of the  $NA$ , which can be achieved with the present technology in lens fabrication. It is

$$\sin \alpha = \frac{D_{\text{eff}}}{2f}, \quad (3)$$

with the effective aperture

$$D_{\text{eff}} = \sqrt{\frac{8R}{\mu N}} \quad (4)$$

The effective aperture is, in general, limited by x-ray attenuation and that is ultimately limited by Compton scattering. The numerical aperture for a given lens material is obtained at that energy, where Compton scattering starts to dominate the mass attenuation. Table 1 gives the values of the resolution for Be, Al, Ni and Pd as lens material when we assume  $R = 100\mu\text{m}$  and  $N = 300$ . These are reasonable parameters which can be realized with the present day technology.

Note that we have optimized the resolution at the expense of the field of view. The imaging, free of distortion, which can be achieved with our rotationally parabolic x-ray lenses has as a prize a relatively large radius of curvature  $R$ . This prevents us from reaching focal lengths in the cm-range which are needed for a lateral resolution in the nm-range. Up to now, a focal length in the cm-range can only be achieved by nanofocusing x-ray lenses.<sup>16,17</sup> They are crossed cylinder lenses with parabolic profile, excellently suited for generating a small focal spot. But there is a prize to be paid: the crossed cylinder geometry makes these lenses not suitable for high quality full field imaging.

	Be	Al	Ni	Pd
$E$ [keV]	15	70	160	250
$f$ [m]	0.134	1.514	2.419	4.830
$D_{\text{eff}}$ [ $\mu\text{m}$ ]	216	207	122	108
$d_t$ [nm]	39	97	115	167

**Table 1.** Optimal lateral resolution  $d_t$  for different lens materials. The energy  $E$  is chosen for each material such that photo absorption and Compton scattering contribute in equal amounts to the attenuation coefficient. The radius of curvature  $R$  is set to  $100\mu\text{m}$  for  $N = 300$  single lenses in the stack. The resulting focal distance  $f$  and the effective aperture  $D_{\text{eff}}$  are also shown.

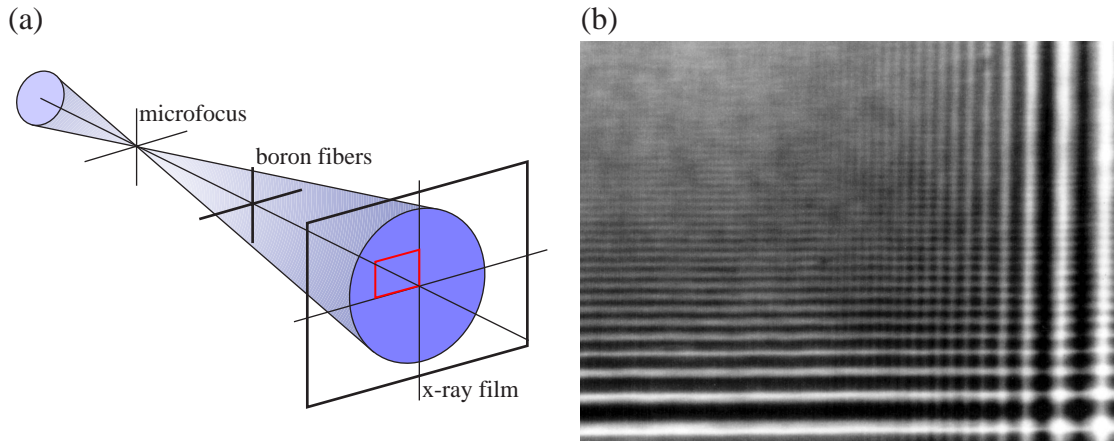


**Figure 8.** (a) Generation of a secondary source of  $0.5\mu\text{m}$  in diameter by means of a parabolic refractive x-ray lens and imaging of two crossed boron fibers with 14.4 keV photons from this secondary source. The distance from the point source to the boron fibers was 766 mm. The high resolution x-ray film was located 1100mm behind the fibers. (b) One quadrant (square in (a)) of the image of the two crossed boron fibers showing more than 20 interference fringes in both directions.

There is a number of other applications for x-ray lenses with rotationally parabolic profile. Magnified tomograms with sub-micrometer resolution were recorded.<sup>18</sup> Full field imaging in demagnifying geometry can be used for hard x-ray lithography.<sup>19</sup>

The high quality of the Al and Be lenses manufactured in Aachen is also demonstrated in the excellent preservation of the lateral coherence by the parabolic refractive lenses. Figure 8 shows the interference fringes by 2 crossed tungsten-boron fibers. A secondary source with  $0.5\mu\text{m}$  in diameter is generated from an ESRF undulator by means of a parabolic lens ( $N = 50$ ,  $f = 0.764\text{mm}$ ,  $E = 14.4\text{keV}$ ). At a distance of  $0.766\text{m}$  this corresponds to a lateral coherence length of about  $66\mu\text{m}$ . More than 20 fringes are visible which shows that the parabolic lenses are excellently suited for imaging in phase contrast and for speckle spectroscopy.

#### 4. MICROFOCUSING WITH PARABOLIC REFRACTIVE X-RAY LENSES

Refractive x-ray lenses with parabolic profile can also be used for generating a sub-micrometer focal spot as used in x-ray analysis and tomography with sub-micrometer resolution. For that purpose, the undulator source is imaged by the lens onto the sample in a strongly demagnifying way, i. e., the source-lens distance  $L_1$  must be much larger than the lens-sample distance  $L_2$ . With Be lenses, we have achieved a spot size of  $1.14\mu\text{m}$  vertically times  $11\mu\text{m}$  horizontally at an ESRF high- $\beta$  undulator, where  $1.1\mu\text{m} \times 11\mu\text{m}$  were expected. At present, the microfocus generated by parabolic refractive x-ray lenses is still limited by geometrical optics. The flux in the focal spot was  $1.05 \cdot 10^{11}\text{ph/s}$ . We can expect a vertical spot size of 100 to 200 nm with our Be lenses, provided all optical compounds in the beamline (like monochromator and mirrors) are mechanically stable. When a small spot size is also required in the horizontal direction, then a low- $\beta$  undulator might be more favorable due to its

smaller horizontal source size. For example, at a distance of  $L_1 = 145\text{m}$  from a low- $\beta$  source at the ESRF (source size  $60\mu\text{m} \times 125\mu\text{m}$  (V $\times$ H), a microbeam of  $220 \times 430\text{nm}^2$  with a gain of  $> 1.2 \cdot 10^6$  is expected. To generate foci in the range of 100nm and below at short distances from the source, focal distances in the centimeter range are needed to generate large demagnifications.<sup>16</sup>

A number of applications have been performed in the meantime which use the small focal size and the large depth of field of microbeams generated by parabolic refractive lenses. They include, for example, microdiffraction,<sup>20</sup> microfluorescence mapping<sup>21</sup> and tomography,<sup>22-24</sup> and x-ray absorption spectroscopic tomography.<sup>25</sup> Be refractive lenses appear to be well suited to focus the beam from an x-ray free-electron-laser.<sup>12</sup>

## ACKNOWLEDGMENTS

The authors would like to thank M. Drakopoulos, and A. S. Simionovici from ESRF, M. Richwin, B. Griesebock and R. Frahm from Wuppertal University and D. R. Haeffner and A. Mashayekhi from Advanced Photon Source for technical and scientific assistance during a number of experiments. The development and fabrication of parabolic refractive x-ray lenses made of beryllium and the development and construction of the x-ray microscope was supported by the German Department of Education and Research (BMBF).

## REFERENCES

1. A. Snigirev, V. Kohn, I. Snigireva, and B. Lengeler, "A compound refractive lens for focusing high energy x-rays," *Nature (London)* **384**, p. 49, 1996.
2. B. Lengeler, J. Tümmler, A. Snigirev, I. Snigireva, and C. Raven, "Transmission and gain of singly and doubly focusing refractive x-ray lenses," *J. Appl. Phys.* **84**(11), pp. 5855-5861, 1998.
3. B. Lengeler, C. G. Schroer, M. Richwin, J. Tümmler, M. Drakopoulos, A. Snigirev, and I. Snigireva, "A microscope for hard x-rays based on parabolic compound refractive lenses," *Appl. Phys. Lett.* **74**(26), pp. 3924-3926, 1999.
4. B. Lengeler, C. Schroer, J. Tümmler, B. Benner, M. Richwin, A. Snigirev, I. Snigireva, and M. Drakopoulos, "Imaging by parabolic refractive lenses in the hard x-ray range," *J. Synchrotron Rad.* **6**, pp. 1153-1167, 1999.
5. B. Lengeler, C. G. Schroer, B. Benner, T. F. Günzler, M. Kuhlmann, J. Tümmler, A. S. Simionovici, M. Drakopoulos, A. Snigirev, and I. Snigireva, "Parabolic refractive X-ray lenses: A breakthrough in X-ray optics," *Nucl. Instrum. Methods A* **467-468**, pp. 944-950, 2001.
6. C. G. Schroer, M. Kuhlmann, B. Lengeler, T. F. Günzler, O. Kurapova, B. Benner, C. Rau, A. S. Simionovici, A. Snigirev, and I. Snigireva, "Beryllium parabolic refractive x-ray lenses," in *Design and Microfabrication of Novel X-Ray Optics*, D. C. Mancini, ed., *Proceedings of the SPIE* **4783**, pp. 10-18, SPIE, (Bellingham), 2002.
7. B. Lengeler, C. G. Schroer, B. Benner, A. Gerhardus, T. F. Günzler, M. Kuhlmann, J. Meyer, and C. Zimprich, "Parabolic refractive X-ray lenses," *J. Synchrotron Rad.* **9**, pp. 119-124, 2002.
8. C. G. Schroer, B. Lengeler, B. Benner, T. F. Günzler, M. Kuhlmann, A. S. Simionovici, S. Bohic, M. Drakopoulos, A. Snigirev, I. Snigireva, and W. H. Schröder, "Microbeam production using compound refractive lenses: beam characterization and applications," in *X-Ray Micro- and Nano-Focusing: Applications and Techniques II*, I. McNulty, ed., *Proceedings of the SPIE* **4499**, pp. 52-63, 2001.
9. B. L. Henke, E. M. Gullikson, and J. C. Davis, "Atomic data and nuclear data tables," 1993.
10. G. Materlik and T. Tschentscher, "TESLA technical design report, part V, the x-ray free electron laser," tech. rep., DESY 2001-011, DESY, Hamburg, 2001.
11. R. M. Bionta, "Controlling dose to low z solids at LCLS," tech. rep., Lawrence Livermore National Laboratory, UCRL-ID-137222, January 3, 2000, LCLS-TN-00-4, 2000.
12. C. G. Schroer, J. Tümmler, B. Lengeler, M. Drakopoulos, A. Snigirev, and I. Snigireva, "Compound refractive lenses: High quality imaging optics for the XFEL," in *X-Ray FEL Optics and Instrumentation*, D. M. Mills, H. Schulte-Schrepping, and J. R. Arthur, eds., *Proceedings of the SPIE* **4143**, pp. 60-68, 2001.



13. C. G. Schroer, B. Benner, M. Kuhlmann, O. Kurapova, B. Lengeler, F. Zontone, A. Snigirev, I. Snigireva, and H. Schulte-Schrepping, "Focusing hard x-ray fel beams with parabolic refractive lenses," in *Fourth Generation X-Ray Sources and Optics II*, S. G. Biedron, W. Eberhardt, T. Ishikawa, and R. O. Tatchyn, eds., *Proceedings of the SPIE* **5534**, 2004. To be published.
14. C. G. Schroer, B. Benner, T. F. Günzler, M. Kuhlmann, B. Lengeler, C. Rau, T. Weitkamp, A. Snigirev, and I. Snigireva, "Magnified hard X-ray microtomography: Toward tomography with sub-micron resolution," in *Developments in X-Ray Tomography III*, U. Bonse, ed., *Proceedings of the SPIE* **4503**, pp. 23–33, 2002.
15. V. Kohn, I. Snigireva, and A. Snigirev, "Diffraction theory of imaging with X-ray compound refractive lens," *Opt. Commun.* **216**, pp. 247–260, 2003.
16. C. G. Schroer, M. Kuhlmann, U. T. Hunger, T. F. Günzler, O. Kurapova, S. Feste, F. Frehse, B. Lengeler, M. Drakopoulos, A. Somogyi, A. S. Simionovici, A. Snigirev, I. Snigireva, C. Schug, and W. H. Schröder, "Nanofocusing parabolic refractive x-ray lenses," *Appl. Phys. Lett.* **82**(9), pp. 1485–1487, 2003.
17. C. G. Schroer, M. Kuhlmann, O. Kurapova, U. T. Hunger, T. F. Günzler, S. Feste, B. Lengeler, S. Ziegler, M. Drakopoulos, A. Somogyi, M. Burghammer, C. Riekel, A. Snigirev, and I. Snigireva, "Nanofocusing parabolic refractive x-ray lenses," in *Design and Microfabrication of Novel X-Ray Optics II*, A. S. Snigirev and D. C. Mancini, eds., *Proceedings of the SPIE* **5539**, 2004. To be published.
18. C. G. Schroer, J. Meyer, M. Kuhlmann, B. Benner, T. F. Günzler, B. Lengeler, C. Rau, T. Weitkamp, A. Snigirev, and I. Snigireva, "Nanotomography based on hard x-ray microscopy with refractive lenses," *Appl. Phys. Lett.* **81**(8), pp. 1527–1529, 2002.
19. C. G. Schroer, B. Benner, T. F. Günzler, M. Kuhlmann, C. Zimprich, B. Lengeler, C. Rau, T. Weitkamp, A. Snigirev, I. Snigireva, and J. Appenzeller, "High resolution imaging and lithography with hard x-rays using parabolic compound refractive lenses," *Rev. Sci. Instrum.* **73**(3), p. 1640, 2002.
20. O. Castelnau, M. Drakopoulos, C. G. Schroer, I. Snigireva, A. Snigirev, and T. Ungar, "Dislocation density analysis in single grains of steel by X-ray scanning microdiffraction," *Nucl. Instrum. Methods A* **467-468**, pp. 1245–1248, 2001.
21. S. Bohic, A. Simionovici, A. Snigirev, R. Ortega, G. Devès, D. Heymann, and C. G. Schroer, "Synchrotron hard x-ray microprobe: Fluorescence imaging of single cells," *Appl. Phys. Lett.* **78**, pp. 3544–3546, 2001.
22. A. S. Simionovici, M. Chukalina, C. Schroer, M. Drakopoulos, A. Snigirev, I. Snigireva, B. Lengeler, K. Janssens, and F. Adams, "High-resolution x-ray fluorescence microtomography of homogeneous samples," *IEEE Trans. Nucl. Sci.* **47**(6), pp. 2736–2740, 2000.
23. C. G. Schroer, J. Tümmeler, T. F. Günzler, B. Lengeler, W. H. Schröder, A. J. Kuhn, A. S. Simionovici, A. Snigirev, and I. Snigireva, "Fluorescence microtomography: External mapping of elements inside biological samples," in *Penetrating Radiation Systems and Applications II*, F. P. Doty, H. B. Barber, H. Roehrig, and E. J. Morton, eds., *Proceedings of the SPIE* **4142**, pp. 287–296, 2000.
24. C. G. Schroer, "Reconstructing x-ray fluorescence microtomograms," *Appl. Phys. Lett.* **79**(12), pp. 1912–1914, 2001.
25. C. G. Schroer, M. Kuhlmann, T. F. Günzler, B. Lengeler, M. Richwin, B. Griesebock, D. Lützenkirchen-Hecht, R. Frahm, E. Ziegler, A. Mashayekhi, D. Haeffner, J.-D. Grunwaldt, and A. Baiker, "Mapping the chemical states of an element inside a sample using tomographic x-ray absorption spectroscopy," *Appl. Phys. Lett.* **82**(19), pp. 3360–3362, 2003.